ARID ZONE JOURNAL OF ENGINEERING, TECHNOLOGY & ENVIRONMENT
AZOJETE June 2026. Vol.22(2):302-315
Published by the Faculty of Engineering, University of Maiduguri, Maiduguri, Nigeria.
Print ISSN: 1596-2490, Electronic ISSN: 2545-5818
https://doi.org/10.63958/AZOJETE/2026/22/02/009
www.azojete.com.ng

ORIGINAL RESEARCH ARTICLE

DEVELOPMENT AND PROPERTIES CHARACTERIZATIONS OF SHEA NUTSHELL ASH (SNSA) REINFORCED ALUMINIUM METAL MATRIX COMPOSITE

A. Gana*, E. O. Onche, I. S. Arudi, O. B. Oloche

Department of Mechanical Engineering, University of Abuja
Corresponding author's email: abdulgana76@yahoo.com

ARTICLE INFORMATION

Received: 21st February 2026
Revised: 7th May 2026
Accepted: 7th May 2026

Keywords:
Composites
Impact
Microstructure
Reinforcement
SEM
Shea nut

ABSTRACT

Growing interest in sustainable and low-cost engineering materials has encouraged the use of agricultural waste as reinforcement in aluminium metal matrix composites. In this study, shea nut shell ash (SNSA), an abundant agro-waste material was used as reinforcement in AA6061 aluminium alloy to develop an environmentally sustainable composite. The composites were produced using the stir casting technique with SNSA additions of 0, 5, 10, 15, 20, 25 and 30 wt%. Microstructural and phase characterisation were carried out using scanning electron microscopy with energy dispersive spectroscopy and X ray diffraction, while mechanical properties were evaluated through tensile, hardness and impact tests in accordance with ASTM standards. The results showed that SNSA is predominantly carbon based with 88.15 wt% carbon and 7.75 wt% oxygen, while minor elements such as Fe 2.18 wt%, Si 0.36 wt% and Ca 0.31 wt% were also detected. X ray diffraction revealed the presence of hard phases including Fe_3C and MnO together with graphite. In addition, the Mechanical properties revealed that the unreinforced AA6061 alloy exhibited the highest tensile strength of 119.77 MPa and elongation of 12.91%. With increasing reinforcement content, tensile strength decreased to 83.04 MPa at 5 wt% and further to 32.32 MPa at 25 wt%, before slightly recovering to 66.56 MPa at 30 wt%. Conversely, hardness increased from 7.6 HRB for the base alloy to a maximum of 13.5 HRB at 30 wt% SNSA. However, the impact energy improved from 2.64 J for the matrix alloy to 8.33 J at 10 wt% reinforcement and remained above the base alloy for all reinforced samples. Furthermore, the results indicate that moderate SNSA additions of 5 to 15 wt% provided the most balanced combination of hardness, strength and impact resistance. Therefore, the study demonstrates that SNSA is a promising sustainable reinforcement for aluminium matrix composites suitable for cost sensitive engineering applications.

1.0 Introduction

Metal matrix composites have attracted sustained research and industrial interest because of their ability to deliver superior mechanical and functional performance, including high strength to weight ratio, improved wear resistance, and enhanced thermal stability. Among these materials, aluminium metal matrix composites are particularly attractive for aerospace, automotive, and defence applications owing to the low density, good corrosion resistance, and favourable processing characteristics of aluminium (Repeto *et al*., 2020). The incorporation of ceramic reinforcements such as silicon carbide, aluminium oxide, boron carbide, and titanium carbide has been widely reported to significantly improve the mechanical properties of aluminium alloys, including hardness, tensile strength, and resistance to wear (Bahera *et al*., 2011; Srinivasan *et al*., 2012; Siddappa *et al*., 2017).

Despite these performance benefits, conventional ceramic reinforcements are often associated with high material cost, increased composite density, and severe tool wear during secondary manufacturing operations. These drawbacks have limited their broader industrial adoption, particularly in cost sensitive and sustainability driven applications (Kok, 2008; Repeto *et al*., 2020). As a result, recent research efforts have increasingly focused on the development of alternative reinforcement materials that are both economical and environmentally sustainable, with particular attention given to agro waste derived resources (Osunmakinde *et al*., 2023; Al-Naib, 2026).

Agricultural waste-based reinforcements such as rice husk ash, coconut shell ash, and shea nut shell ash (SNSA) have gained growing attention due to their wide availability, low cost, and reduced environmental impact (VenkataSiva *et al*., 2013; Baradeswaran and Elayaperumal, 2014). Among these materials, SNSA has emerged as a promising bio-based reinforcement for aluminium metal matrix composites. Interestingly, SNSA is rich in silica and alumina, its oxides contribute positively to improve strength and wear resistance mechanisms in aluminium based composites (Pooja *et al*., 2025).

However, when compared with extensively studied reinforcements such as silicon carbide and aluminium oxide, studies on SNSA reinforced aluminium metal matrix composites remain relatively limited (Koraa and Gorantla, 2023; Alaneme and Adewuyi, 2013). Existing investigations have primarily focused on selected property evaluations, while only few offering a systematic examination of the combined mechanical response and microstructural characteristics across varying processing conditions and reinforcement contents (Sharma *et al*., 2021; Sharma *et al*., 2024). Thus, further experimental evidence is required to support a broader assessment of SNSA as a reinforcement material for aluminium based composites.

Among the various fabrication routes available for aluminium metal matrix composites, stir casting remains the most widely adopted liquid state processing technique due to its simplicity, cost effectiveness, and suitability for large scale production (Das *et al*., 2018; Thandalam *et al*., 2015). Previous studies have demonstrated that stir casting can successfully produce aluminium composites reinforced with conventional ceramic particles, provided that challenges such as particle agglomeration, porosity, and weak interfacial bonding are adequately controlled through careful process optimisation (Kumar and Devi, 2020; Pandey and Dwivedi, 2024). The application of this technique to SNSA reinforced systems, therefore, warrants a thorough systematic investigation.

While machinability is an important consideration for the practical deployment of aluminium metal matrix composites, existing studies on conventionally ceramic-reinforced composites have shown that hard reinforcement particles strongly influence cutting forces, surface quality, and tool wear (Repeto *et al*., 2020; Bai *et al*., 2019). These findings provide motivation for exploring alternative reinforcement materials such as SNSA, to see its potential for industrial application.

Against this background, the present study focuses on the development and mechanical investigation of SNSA reinforced aluminium metal matrix composites produced via stir casting. Emphasis is placed on the evaluation of microstructural features and mechanical properties in order to establish the strengthening potential of SNSA as a sustainable reinforcement material.

2. Materials and Method

2.1 Materials

The primary materials used in this study are aluminium alloy as the matrix material and SNSA as the reinforcing phase. The aluminium alloy selected is AA6061, chosen for its favourable mechanical properties, good corrosion resistance, and excellent machinability. The SNSA was obtained from locally sourced shea nut shells in Bida, Niger State, and processed into ash for use as a reinforcement material. The selection of SNSA is motivated by its low density, wide availability, and strong potential as a sustainable and cost-effective reinforcement for aluminium matrix composites.

2.2 Equipment

The following major equipment were utilized for this study:

1. Muffle Furnace (Carbolite CWF 1200)

Corresponding author's email address: abdulgana76@yahoo.com

2. Furnace
3. Stir casting apparatus
4. X-ray Fluorescence (XRF) Analyzer (Bruker S8 TIGER)
5. Charpy Impact testing machine (Capacity 15-25 joules), serial No. 412-07-15269C
6. Phenol proX scanning electron microscope (SEM) EVO MA-10, equipped with energy dispersive x-ray (EDX) analyser
7. Universal Testing Machine (Instron 5982, 100 kN capacity)
8. Lathe Machine
9. Profilometer (Mitutoyo Surftest SJ-410)
10. Optical Microscope (Leica DM750M)

2.3 Method

2.3.1 Matrix material

Aluminium 6061 alloy was used to make the metal matrix composite. Al 6061-T6 alloy (Al 95.85-98.56%), is a medium to high strength heat treatable alloy. It has good corrosion resistance and weldability. The mechanical properties of this metal can be enhanced by adding tough reinforcements into the aluminium metal matrix. XRF was conducted on the sourced sample to determine its elemental composition.

2.3.2 Reinforcement material

Shea nut shell (SNS) was obtained locally from Bida local government, Niger State. It is an agricultural waste product obtained from Shea nut when the nut is removed. These shells are rich in organic and inorganic compounds, and after combustion, they primarily contain oxides such as silica (SiO_2), alumina (Al_2O_3), iron oxide (Fe_2O_3), and other trace elements.

2.3.3 Preparation of shea nut shell ash (SNSA)

The shell which is the desired material was obtained after the nut is removed/separated from the shea nut. After obtaining the shell, it was washed to remove the impurities and then sun dried for two days. The dried SNS was then milled using a THOMAS willey mill, model ED-5 milling machine shown in Plate 1(a). The milled samples were then sieved with 250 µm mesh sieve to obtain a fine particle size according to ASTM E11-20 (Zubairu *et al*., 2021).

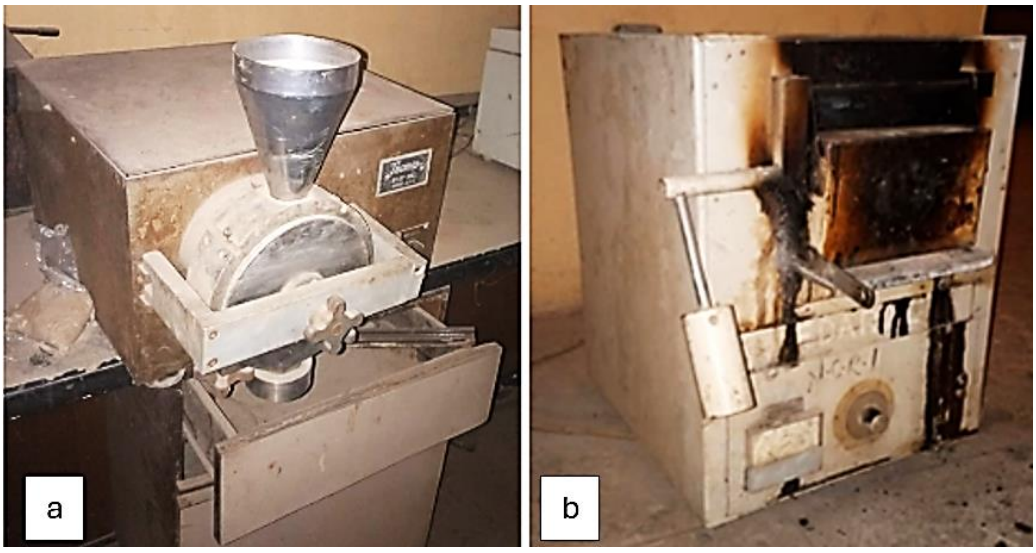

Plate 1: a. Milling machine for milling samples, b. Muffle furnace used for SNS carburisation

The SNSA was produced by controlled combustion of shea nut shells in the muffle furnace shown in Plate 1(b) at 700°C for 4 hours. Before combustion, the shea nut shells will be dried at 110°C for 24 hours in a hot air oven to remove moisture.

Corresponding author's email address: abdulgana76@yahoo.com

The combustion process follows a slow heating rate of 5 °C/min to prevent sudden thermal degradation and minimize impurities. The resulting ash was ground for 2 hours to achieve a fine and homogeneous particle distribution. After grinding, the ash was sieved using a 50 µm mesh sieve according to ASTM E11 standard, to obtain uniform reinforcement particles suitable for dispersion in the aluminium matrix. Similar method was reported by Saraki *et al.* (2025). The composition of SNSA was analysed using XRF and SEM to determine the elemental constituents and morphology of the particles.

2.3.4 Composite fabrication

The fabrication of the AMMC reinforced with SNSA was carried out using the stir casting method to ensure uniform dispersion of the reinforcement particles. The process began with the melting of the aluminium alloy (AA6061) in the furnace (Figure 3.2) at 750°C, using a graphite crucible to prevent contamination. The melt was maintained at this temperature for 20 mins to ensure complete liquefaction.

The SNSA particles was preheated at 300°C for 1 hour to remove moisture and improve wettability with the molten aluminium. A mechanical stirrer equipped with a graphite-coated impeller was used to create a vortex in the molten aluminium at a stirring speed of 500 rpm for 10 mins in 30 s intervals. The preheated SNSA particles was gradually introduced into the vortex at a controlled feed rate to ensure uniform dispersion and minimize particle agglomeration. To enhance bonding between the matrix and reinforcement, magnesium (Mg) at 1 wt% was added to the melt as a wetting agent.

Once the stirring process was complete, the composite melt was poured into a preheated steel mould and allowed to solidify and cool at room temperature. The solidified composite samples were then machined into standard test specimens for subsequent mechanical, machining, and microstructural analysis. The reinforcement was added in 5, 10, 15, 20, 25 and 30 wt% as shown in Table 1.

Table 1: Composite fabrication formulations

Samples	Composition	
	Aluminium matrix (%)	SNSA Reinforcement (%)
S1	100	0
S2	95	5
S3	90	10
S4	85	15
S5	80	20
S6	75	25
S7	70	30

2.3.5 Mechanical tests procedure

The mechanical properties such as tensile test, hardness test, impact energy and wear tests of the composites were determined according to ASTM standards.

Tensile test

Tensile test specimens were prepared in accordance with ASTM E8/E8M standard test methods for tension testing of metallic materials. Each specimen had a diameter of 8 mm and a gauge length of 60 mm. The specimens were tested using a Hounsfield tensiometer. For the tensile test, each specimen was mounted in the testing machine, and an extensometer was attached to measure deformation. Tensile load was then applied at a constant loading rate of approximately 2 mm/min until the specimen fractured, with fracture loads in the range of about 1.6 to 6.0 kN depending on the sample. The maximum load recorded at fracture was noted, and the corresponding force per unit original cross-sectional area was calculated to determine the tensile strength of the sample.

Hardness test

Identec universal hardness testing machine: MODEL 8187.5KV (B), Indenter; Diamond cone (120°), Scale A was used to determine the hardness properties of the developed composites in accordance with ASTM E384-11 standards. A load of 1N for a period of 10 s was applied on specimens. The hardness was determined by recording the diagonal lengths of indentation produced. The test was carried out at three different points on the specimens and the average value taken as the hardness of the cast specimens.

Corresponding author's email address: abdulgana76@yahoo.com

Impact test

The impact test was conducted in accordance with ASTM E 602-91 standard method and definitions for mechanical testing of steel products. V-notches of 0.5mm depth was made on the samples each and the impact strength carried out using Hounsfield balance Impact testing machine (Joules). Charpy Impact testing machine (Capacity 15-25 Joules) was used to carry out the test on the samples.

Wear test

The wear test was performed using a pin-on-disk tribometer following ASTM G99 to evaluate the tribological performance of the SNSA-reinforced aluminium composite. Composite pins (Ø10 mm × 30 mm) were tested against a rotating hardened steel disk under varying loads (10 N, 20 N, 30 N) and sliding speeds (200 rpm, 400 rpm, 600 rpm), with a constant sliding distance of 1000 m.

The specimens were weighed before and after testing using a high-precision balance to determine weight loss, and the wear rate was calculated. The worn surfaces were examined using SEM to analyse wear mechanisms such as abrasion, adhesion, and delamination.

2.3.6 Microstructural analysis

Before the metallography and surface morphology examination, the surface of the samples was successively grounded using grit papers of different grades 12 °C, 18 °C, 32 °C, 40 °C, 60 °C, 80 °C and 120 °C. Being aluminium, grinding was carried out from the 40 °C grit paper to the 120 °C grit paper with the application of lubricant intermittently; this is to prevent overheating and provides a rinsing action, which flushes away the particles being removed from the surface. They were subsequently polished with the aid of a polishing machine using alumina to remove the scratches that are left during grinding. Etching was then carried out, which is the chemical attack on the surface of a polished metal, the etchant used for aluminium samples are "Keller's reagent, which is a solution of 1 ml distilled water, 5 ml nitric acid and 2 ml hydrofluoric acid. A computerised photographic visual metallurgical microscope, MODEL NJF-120 A, rating 230 V-5 V/60 Hz was then used to view the microstructures of the polished samples.

3. Results and Discussion

3.1 Characterisation of Control Sample

Prior to the development of the Shea Nut Shell Ash (SNSA) reinforced aluminium metal matrix composites, the control sample was characterised to establish the baseline properties of the unreinforced aluminium alloy

3.1.1 X-ray fluorescence (XRF) result for AA6061

Table 1 presents the X-ray Fluorescence (XRF) result for the control sample to ascertain its elemental composition unaffected by surface contamination.

Aluminium was measured at 97.46 wt%, clearly confirming the alloy's dominant constituent. Other major elements detected include Fe at 0.686 wt%, Si at 0.678 wt% and Mn 0.519 wt%. Additional alloying or trace elements include Cu, Sc and Ca. The values obtained are similar to results obtained by Abbas and Sharhan (2023) (Fe at 0.586 wt%, Si at 0.636 wt% and Mn 0.105 wt%). The Mn content (0.519 wt.%) is higher than the standard specification for 6061 aluminium alloy as stated by Abbas and Sharhan (2023) which is 0.15 wt%, suggesting the material may originate from recycled or modified alloy stock. Overall, the sample falls within the typical compositional range specified for AA6061, where aluminium generally exceeds 95 wt%, and silicon and magnesium form the primary strengthening phases as stated by Tsaknopoulos *et al.* (2022) and Kareem *et al.* (2021).

3.1.2 SEM-EDS result for AA6061

SEM examination revealed a metallic matrix with regions of contrasting brightness as depicted in Figure 2. These contrast differences are typically associated with compositional variations, where heavier elements form brighter regions under backscattered electron imaging. The micrographs showed the presence of

Corresponding author's email address: abdulgana76@yahoo.com

dispersed intermetallic particles embedded within the aluminium matrix features characteristic of AA6061 alloys.

Table 1: X-ray Fluorescence (XRF) results for AA6061

Compound	Conc. Unit (m/m%)
Al	97.4600
Fe	0.68600
Si	0.67800
Mn	0.51900
Cu	0.18600
Sc	0.09420
Ca	0.07540
Ni	0.06430
Cr	0.05620
Cl	0.05400
S	0.02830
K	0.02300
Pb	0.02020
Tl	0.01640
Ti	0.01490
Sn	0.01370
Mo	0.01010
Na	0.04200
Co	0.01000
Cs	0.00190
Rb	0.00170
Ag	0.00051
Nb	0.00029

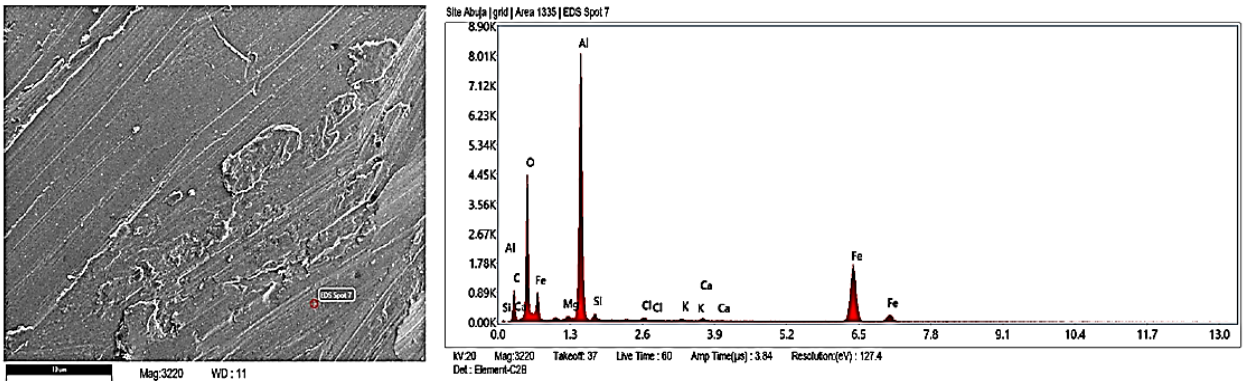

Figure 2: SEM for AA 6061, b. EDS for AA 6061

Surface scratches and polishing marks are also visible in the micrograph, indicating the mechanical preparation process applied during sample polishing. These features may introduce localized surface contamination, which can influence the elemental signals detected during EDS analysis and is reflected in the elemental composition presented in Table 2.

The EDS spectrum in Figure 2 is dominated by a strong aluminium peak, confirming that aluminium is the principal constituent of the alloy. This observation is consistent with the established composition of AA6061 alloys, where aluminium typically constitutes more than 95 wt.% of the material. Kareem *et al.* (2021) similarly reported aluminium as the dominant element in their compositional analysis of AA6061 alloys. Distinct peaks for Mg and Si are also observed; the two elements are the primary alloying constituents in 6061. They are responsible for the formation of the strengthening Mg_2Si phase during heat treatment as stated by Atanacio-Sánchez *et al.* (2024). Minor peaks associated with iron are detected at several energy levels, suggesting the presence of Fe-rich intermetallic compounds within the microstructure. These phases

commonly occur as impurity-related particles in commercial aluminium alloys and have been reported in previous microstructural investigations of 6061 alloys by Que *et al.* (2018).

Small signals corresponding to O and C are also present in the EDS spectrum. These elements are typically associated with surface oxidation of aluminium or environmental contamination during specimen preparation and SEM examination. Interestingly, some very weak peaks corresponding to K, Ca, and Cl are detected as well. Their extremely low intensities indicate that they are most likely related to residual surface contaminants, polishing compounds, or background instrumental effects rather than intentional alloying additions, as noted in the SEM–EDS analysis reported by Zhang *et al.* (2023).

3.1.3 X-ray diffraction (XRD) result of AA6061

Figure 3 presents the X-ray diffraction (XRD) pattern of the AA6061 aluminium alloy sample obtained using Co Kα radiation. The diffractogram is dominated by the characteristic reflections of face-centred cubic (FCC) aluminium, with major peaks observed at approximately 45°, 52°, and 77° 2θ, corresponding to the 111, 200, and 220 crystallographic planes, respectively. These are similar to results reported by Gassour *et al.* (2023) of which are brag reflections were noticed for 2θ values at 38.4°, 44.6° and 64.76° that correspond to 111, 200 and 220 lattice planes diffractions, respectively.

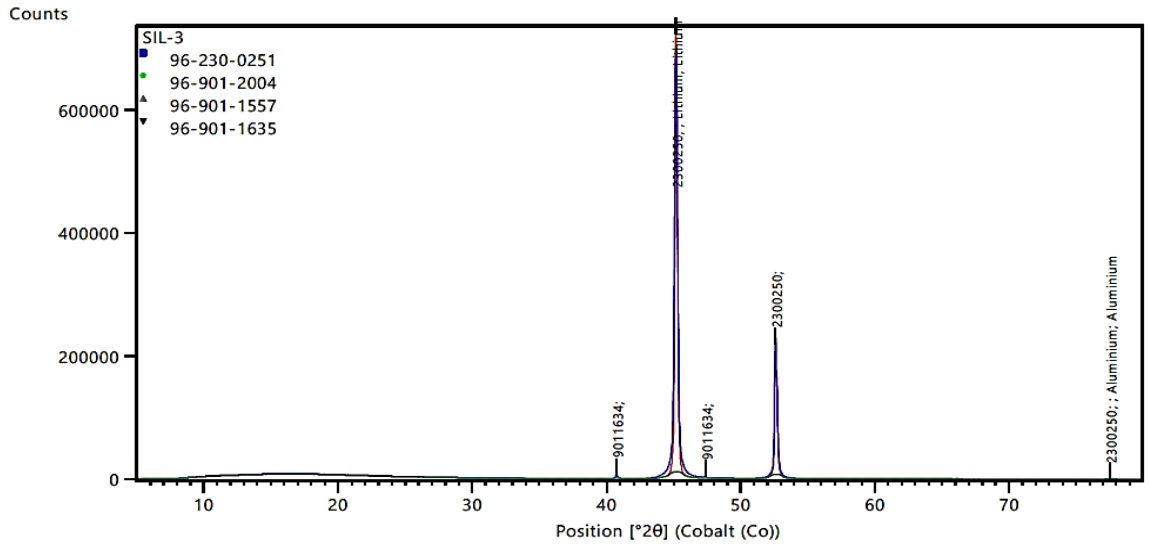

Figure 3: XRD for AA6061

These intense and well-defined peaks confirm that aluminium is the primary phase present in the alloy. A few low-intensity peaks appear between 40° and 50° 2θ, which are attributed to minor secondary phases typically associated with AA6061, such as Mg–Si or Al–Fe–Si intermetallics that form during alloy processing with similar results from Gassour *et al.* (2023). Overall, the XRD profile indicates a predominantly aluminium matrix with small amounts of alloying-element precipitates, which is consistent with the known metallurgy of AA6061.

3.2 Microstructural and Chemical Characterisation of the SNSA

The microstructural and chemical characterisation of the SNSA was undertaken to establish its suitability as reinforcement for AA6061 aluminium matrix composite production. Since the strengthening behaviour of any particulate reinforcement is strongly dependent on its elemental composition and crystalline phases, both SEM–EDS and XRD analyses were used to determine the chemical constituents and mineralogical structure of the ash. These results provide the necessary foundation for understanding the interaction between SNSA and the aluminium matrix, as well as the mechanical performance of the resulting composites.

3.2.1 SEM–EDS Analysis

The microstructural features observed in the SEM micrograph presented in Figure 4 show that the SNSA consists predominantly of irregular, angular and plate-like particles with distinctly rough surface textures similar to micrograph presented by Musah *et al.* (2024).

Corresponding author's email address: abdulgana76@yahoo.com

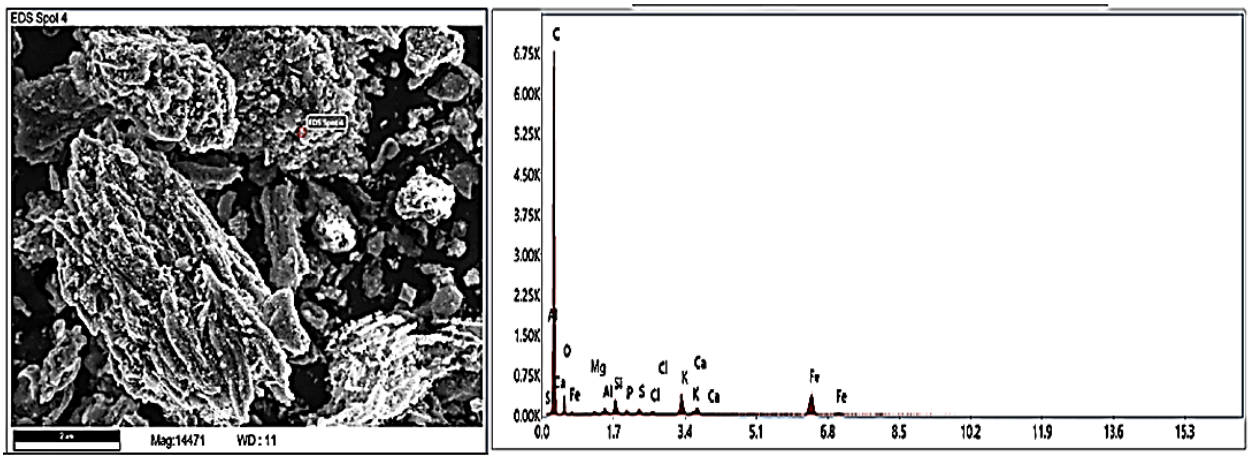

Figure 4: SEM-EDS for SNSA

This morphology is advantageous during composite fabrication because the irregular geometry promotes stronger mechanical interlocking with the aluminium matrix, while the surface roughness enhances the potential for improved particle–matrix bonding as opined by Odoni *et al.* (2024).

The chemical composition of the SNSA, as revealed by the EDS spectrum in Figure 4, shows that the material is overwhelmingly carbonaceous, with a very high-intensity C peak dominating the spectrum. This indicates successful carbonization of the shea nut shell precursor and suggests that the ash contains a high proportion of amorphous or partially graphitized carbon. O is the second most significant element detected, reflecting the presence of oxide phases formed during carbonization. Several minor but distinct peaks corresponding to Mg, Al, Si, S, P, Cl, K, Ca and Fe are also present, indicating the mineral-rich nature of the ash. These elements correspond to naturally occurring inorganic constituents in plant biomass and their oxides typically contribute to hardness, stiffness and thermal stability in composite applications. The appearance of iron peaks at higher energies, including around 6.4–7.0 keV, suggests the presence of iron-bearing phases which can be beneficial in enhancing the wear performance of aluminium-based composites as observed from the study conducted by Christy *et al.* (2010).

The quantitative results in Table 3 support the qualitative information obtained from the EDS spectrum. C accounts for 88.15 wt%, confirming that the material is predominantly carbon-based. The high carbon content is desirable for lightweight composite reinforcement and contributes to improved thermophysical stability during the aluminium casting process. O represents 7.75 wt% of the total composition, indicating the presence of oxide structures such as SiO_2, CaO, MgO and Al_2O_3 as also obtained in results of Frías *et al.* (2011). Although present only in small fractions, these oxides collectively play a significant role in strengthening mechanisms once the ash is incorporated into the AA6061 matrix, as their inherent hardness and thermal stability can contribute to improved mechanical performance as stated by Frías *et al.* (2011).

Table 3: Quant result for SNSA SEM-EDS

Element	Weight (%)
C K	88.15
O K	7.75
Mg K	0.09
Al K	0.16
Si K	0.36
P K	0.06
S K	0.11
Cl K	0.05
K K	0.79
Ca K	0.31
Fe K	2.18

Minor mineral constituents such as Si, Mg, K, Ca, P, S and Cl occur in trace amounts, but their presence is consistent with compositions of other biomass-derived ashes, like rice husk ash, palm oil ash and coconut shell ash as reported by Joseph and Babaremu (2019). Fe constitutes 2.18 wt% and, though relatively small, this amount is sufficient to introduce harder phases that can positively influence the composite's wear and abrasion behaviour.

Corresponding author's email address: abdulgana76@yahoo.com

3.2.2 XRD analysis

X ray diffraction analysis shows that SNSA contains a diverse combination of crystalline and amorphous phases that explain its effectiveness as a reinforcement for AA6061. Five major crystalline phases were identified: cohenite Fe3C, manganosite MnO, schreibersite iron nickel phosphide, graphite, and freibergite, as shown in Figure 5.

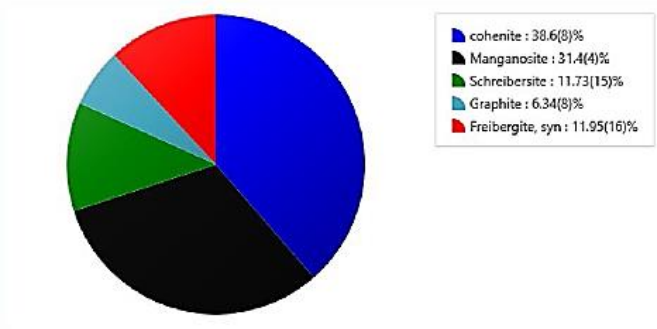

Figure 5: SNSA XRD plot

Cohenite is the dominant phase at 38.6% and confirms strong iron carbon interactions during high temperature processing. As a hard and wear resistant iron carbide, it is expected to significantly improve hardness and load bearing capacity of the composite based on studies conducted by Bhadeshia (2020). Manganosite accounts for 31.4% of the phases and reflects the manganese rich nature of the biomass. Its high thermal stability and strengthening capability suggest improved hardness and elevated temperature performance as concluded in a study conducted by Ghosh (2020).

The XRD pattern also shows a moderate amorphous background associated with non-crystalline carbon formed during partial combustion. This combination of hard crystalline phases and softer carbonaceous material is typical of bio waste ashes. It is beneficial for balancing strength, wear resistance, and energy absorption as observed by Wang and Zhang (2023). Overall, SNSA can be described as a hybrid reinforcement consisting of a carbon rich matrix enriched with hard ceramic and metallic phases. This structure is well suited for aluminium matrix composites, where carbon enhances wear resistance while iron and manganese-based phases contribute to hardness, strength, and possible grain refinement during AA6061 solidification.

3.4 Mechanical Tests Results

This section presents and discusses the mechanical behaviour of the aluminium 6061–SNSA composite samples. The mechanical tests conducted include tensile testing, hardness measurement and impact toughness evaluation. The results are examined in relation to increasing reinforcement content (0–30% SNSA), in order to understand the influence of the reinforcement phase on the composite's mechanical performance.

3.4.1 Tensile test results

Figure 6 presents the tensile test results for the developed composites. It shows clear variations in mechanical performance across the seven samples. The unreinforced control sample S1 of AA6061 matrix recorded the highest tensile strength of 119.77 MPa, an elastic modulus of 719.62 MPa, and a total elongation of 12.905%. These values reflect the intrinsic ductility and moderate strength of heat-treatable AA6061.

Upon incorporation of SNSA reinforcement, the tensile strength initially decreases significantly as depicted in Figure 6. Sample S2, containing 5% reinforcement, shows a reduction to 83.04 MPa, while the modulus drops to 492.56 MPa and elongation reduces to 11.63%. A similar trend were observed for S3 and S4 with 97.60 MPa and 93.20 MPa respectively, both of which exhibit lower strengths than the pure matrix. This is similar to behaviour obtained by Zubairu *et al.* (2021) that recorded reduction in tensile strength with addition of SNSA reinforcement.

Corresponding author's email address: abdulgana76@yahoo.com

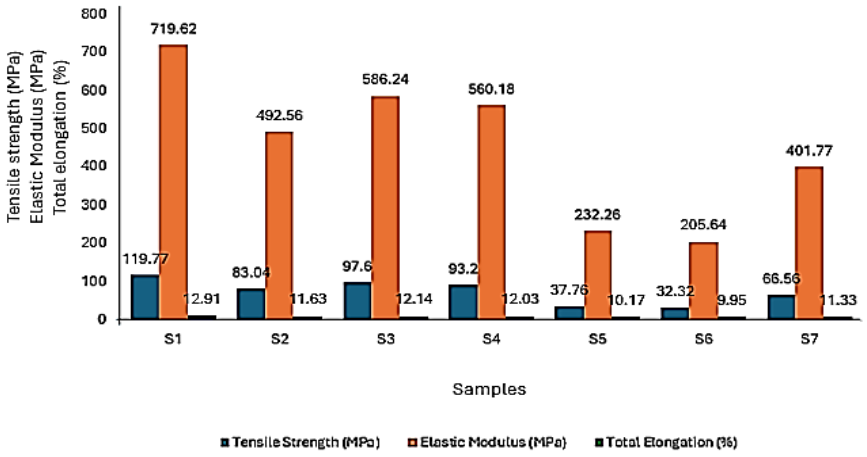

Figure 6: Tensile test results

The decline in tensile strength with increasing reinforcement content up to 15% can be attributed to two primary factors. First, the introduction of rigid ceramic-like SNSA particles reduces the continuity of the metallic matrix, which impairs load transfer uniformity and introduces potential stress concentration points. Second, the interfacial bonding between the aluminium matrix and the SNSA reinforcement may hinder efficient stress transfer during deformation as observed in studies by Pooja *et al.* (2025) and Balokhonov *et al.* (2022).

A more remarkable deterioration is observed in samples with high reinforcement contents. Samples S5 and S6 show very low tensile strengths of 37.76 MPa and 32.32 MPa, respectively, accompanied by substantial reductions in stiffness (232.26 MPa and 205.64 MPa). These pronounced declines indicate that excessive reinforcement loading leads to poor matrix–particle cohesion, particle agglomeration and microvoid formation, all of which weaken the composite as asserted by Pooja *et al.* (2025). Even at 30% reinforcement in sample S7, tensile strength partially recovers to 66.56 MPa, though still far below the performance of the unreinforced sample. The partial improvement at 30% may result from better distribution of reinforcement at this loading compared with the transitional levels of 20 and 25%, though the matrix remains significantly weakened overall.

The total elongation values support this interpretation. All reinforced samples exhibit lower elongation than the pure matrix, with values ranging from 9.945% to 12.135% as seen in Figure 6, indicating reduced ductility associated with ceramic particle incorporation, which is similar to results obtained by Pooja *et al.* (2025). The lowest elongation is observed in S6 with value of 9.945%, corresponding to the highest brittleness caused by excessive reinforcement.

3.4.2 Hardness test results

The hardness results show a trend opposite to that of tensile strength as shown in Figure 7. The hardness of the pure AA6061 sample S1 is 7.6 HRB, which increases upon reinforcement addition. Samples S2 through S7 record hardness values of 11.0, 12.66, 11.2, 10.96, 11.43, and 13.5 HRB, respectively.

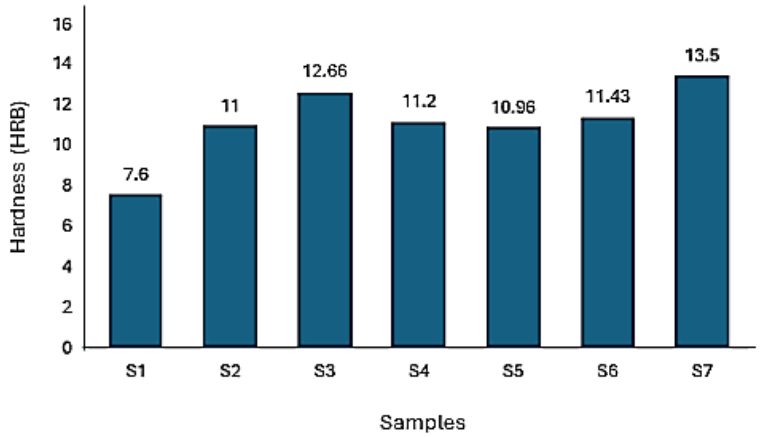

Figure 7: Hardness test results

Corresponding author's email address: abdulgana76@yahoo.com

The highest hardness value is observed in S7 with 30% reinforcement and 13.5 HRB, representing almost a two-fold increase relative to the pure matrix which is similar to results obtained by Zubairu *et al.* (2021). This steady increase in hardness with higher reinforcement content is expected, as the hard SNSA particles restrict plastic deformation of the soft aluminium matrix. The particles act as obstacles to dislocation motion, increasing the composite's resistance to indentation.

The slight drop in hardness for intermediate samples like in S4 and S5 may be due to clustering of reinforcement particles, which creates non-uniform strengthening and locally weak zones as depicted in results obtained by Kumar and Sultan (2015) and Ghandvar *et al.* (2017). However, the overall trend clearly shows that hardness improves with SNSA addition, particularly at higher reinforcement fractions.

3.4.3 Impact test results

The impact test results reveal important complementary information as shown in Figure 8. Sample S1 has an impact energy of 2.64 J, which increases significantly to 5.45 J for S2 and further to 8.33 J for S3. Sample S4 also maintains a relatively high value of 7.6 J, demonstrating that low to moderate reinforcement levels of 5 to 15% improve the impact resistance of the composite.

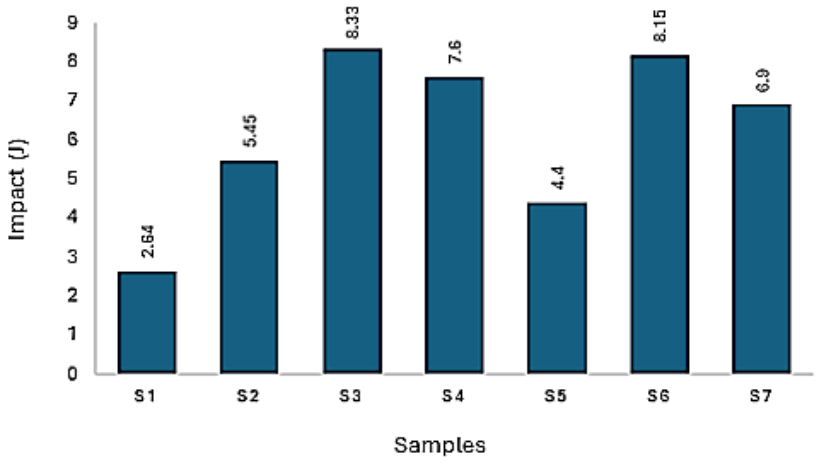

Figure 8: Impact test results

This improvement suggests that SNSA particles may act to deflect crack propagation paths, increasing the energy absorbed before fracture. However, at higher reinforcement contents, the toughness begins to decline again. S5 and S7 record impact strengths of 4.4 J and 6.9 J, respectively, while S6 shows 8.15 J, indicating a non-linear response. The slight recovery at 30% reinforcement may be related to better distribution of particles in S7 compared with intermediate levels, where particle clusters may have facilitated brittle fracture.

Despite these variations, none of the reinforced samples exhibit impact energies as low as the pure AA6061 matrix, suggesting that the introduction of small amounts of reinforcement enhances toughness, but very high reinforcement levels can lead to embrittlement depending on dispersion quality.

4. Conclusion

This study successfully developed AA6061 aluminium metal matrix composites reinforced with Shea Nut Shell Ash (SNSA) using the stir casting technique at reinforcement levels of 0–30 wt%. Characterisation of the SNSA confirmed the presence of carbon-rich constituents and hard phases such as Fe_3C and MnO, while the SEM morphology revealed irregular and rough particles capable of promoting effective reinforcement within the aluminium matrix.

The mechanical properties of the composites were significantly influenced by the addition of SNSA. The unreinforced AA6061 alloy exhibited the highest tensile strength of 119.77 MPa and elongation of 12.905%, while the tensile strength of the reinforced composites decreased with increasing SNSA content, reaching 32.32 MPa at 25 wt% reinforcement. Similarly, the elastic modulus reduced from 719.62 MPa for the control

Corresponding author's email address: abdulgana76@yahoo.com

sample to lower values at higher reinforcement levels. This reduction was attributed to particle agglomeration and weakening of matrix continuity at excessive reinforcement contents.

In contrast, hardness improved consistently with increasing SNSA addition. The hardness value increased from 7.6 HRB for the unreinforced alloy to a maximum value of 13.5 HRB at 30 wt% reinforcement, indicating improved resistance to plastic deformation. Impact toughness also improved significantly at moderate reinforcement levels, increasing from 2.64 J for the control sample to 8.33 J at 10 wt% SNSA before fluctuating at higher reinforcement contents.

Overall, the composites containing 5–15 wt% SNSA exhibited the most balanced mechanical performance by combining improved hardness and impact resistance with moderate tensile properties. The findings therefore confirm that SNSA, an agro-waste material, has good potential as a sustainable and cost-effective reinforcement for aluminium matrix composites in engineering applications requiring improved surface hardness and adequate toughness.

References

Abbas, MA. and Sharhan, NAB. 2023. Characteristics of Al6061-SiC-Al2O3 surface hybrid composites fabricated by friction stir processing. Journal of Materials and Engineering, 1(4): 147-158.

Alaneme, K. N., and Adewuyi, E. O. 2013. Mechanical behaviour of Al-Mg-Si matrix composites reinforced with alumina and bamboo leaf ash. *Metallurgical and Materials Engineering*, 19(3): 1-18.

Al-Naib, UM. 2026. Industrial and agro-waste reinforcements in aluminum matrix composites: Toward sustainable materials development. *Total Environment Engineering*, 6: 1-15

ASTM. 2021. ASTM E8/E8M-21: Standard test methods for tension testing of metallic materials. ASTM International.

Atanacio-Sánchez, X., Garay-Reyes, CG., Martínez-García, A., Estrada-Guel, I., Mendoza-Duarte, JM., Guerrero-Seañez, P., González-Sánchez, S., Rocha-Rangel, E., de Jesús Cruz-Rivera, J., Gutiérrez-Castañeda, EJ. and Martínez-Sánchez, R. 2024. Enhancement of the electrical conductivity and mechanical properties of Al-Mg-Si and Al-Mg-Zn ternary systems after a T8 heat treatment. Metals, 14(11): 1-25.

Bahera, R., Das, S., Chatterjee, D. and Sutradhar, G. 2011. Forgeability and machinability of stir cast aluminum alloy metal matrix composites. Journal of Minerals and Materials Characterization and Engineering, 10(10): 923-939.

Bai, W., Roy, A., Sun, R. and Silberschmidt, VV. 2019. Enhanced machinability of SiC-reinforced metal-matrix composite with hybrid turning. Journal of Materials Processing Technology, 268: 149-161.

Balokhonov, RR., Romanova, VA., Buyakova, SP., Kulkov, AS., Bakeev, RA., Evtushenko, EP. and Zemlyanov, AV. 2022. Deformation and fracture behavior of particle-reinforced metal matrix composites and coatings. Physical Mesomechanics, 25: 492-504.

Baradeswaran, A. and Elayaperumal, A. 2014. Study on mechanical and wear properties of Al 7075/Al2O3/graphite hybrid composites. Composites Part B Engineering, 56: 464-471.

Bhadeshia, HK. 2020. Cementite. International Materials Reviews, 65(1): 1-27.

Christy, TV., Murugan, N. and Kumar, S. 2010. A comparative study on the microstructures and mechanical properties of Al 6061 alloy and the MMC Al 6061/TiB2/12p. Journal of Minerals and Materials Characterization and Engineering, 9(1): 57-65.

Das, D., Mishra, PC., Singh, S., Chaubey, AK. and Routara, BC. 2018. Machining performance of aluminium matrix composite and use of WPCA based Taguchi technique for multiple response optimization. International Journal of Industrial Engineering Computations, 9: 551-564.

Corresponding author's email address: abdulgana76@yahoo.com

Frías, M., Villar, E. and Savastano, H. 2011. Brazilian sugar cane bagasse ashes from the cogeneration industry as active pozzolans for cement manufacture. Cement and Concrete Composites, 33: 490-496.

Gassour, H., El-Magd, GEAA., Mazen, A. and Ibrahim, AMM. 2023. Characterization of aluminum composite reinforced by silver nanoparticles. Scientific Reports, 13(1): 1-24.

Ghandvar, H., Idris, MH., Ahmad, N. and Moslemi, N. 2017. Microstructure development, mechanical and tribological properties of a semisolid A356/xSiCp composite. Journal of Applied Research and Technology, 15(6): 533-544.

Ghosh, SK. 2020. Diversity in the family of manganese oxides at the nanoscale: from fundamentals to applications. ACS Omega, 5(40): 25493-25504.

Joseph, OO. and Babaremu, KO. 2019. Agricultural waste as a reinforcement particulate for aluminum metal matrix composite (AMMCs): A review. Fibers, 7(4): 33-40.

Kareem, A., Qudeiri, JA., Abdudeen, A., Ahammed, T. and Ziout, A. 2021. A review on AA 6061 metal matrix composites produced by stir casting. Materials, 14(1): 175-186.

Kok, M. 2008. A study on the machinability of Al2O3 particle reinforced aluminium alloy composite. International Inorganic Bonded Fiber Composites Conferences, 272-281.

Kora, P. L. S. & Gorantla, N. 2023. Study On Behaviour Of Aluminium Metal Matrix Composite Reinforced With Silicon Carbide And Titanium Diboride. *IOP Conference Series Earth and Environmental Science*, 1130(1), 0120-0130

Kumar, K. and Sultan, S. 2015. Effect of electromagnetic field and mechanical milling in the synthesis of metal matrix nano composite. International Journal of Advance Research and Innovation, 3(2): 175-186.

Kumar, PV. and Devi, SB. 2020. Machinability investigation of aluminium based hybrid metal matrix composite. International Journal of Multidisciplinary Research in Science, Engineering and Technology, 3(1): 35-41.

Musah, M., Mathew, JT., Azeh, Y., Badeggi, UM., Muhammad, AI., Abu, LM., Okonkwo, PT. and Muhammad, KT. 2024. Preparation and characterisation of adsorbent waste shea (Vitellaria paradoxa) nut shell. FUDMA Journal of Sciences, 8(2): 338-344.

Odoni, BU., Awheme, O. and Onyekpe, BO. 2024. Evaluation of palm kernel shell ash particle reinforced aluminium 6061 alloy matrix composites using physio-chemical and microstructural methods. Journal of Materials Engineering, Structures and Computation, 3(1): 1-15.

Pandey, A. and Dwivedi, V. 2024. Experimental analysis of machining parameters of metal matrix composite. International Research Journal of Engineering and Technology, 11(4): 575-580.

Pooja, K., Tarannum, N. and Chaudhary, P. 2025. Metal matrix composites: revolutionary materials for shaping the future. Discover Materials, 5(35): 1-19.

Que, Z., Wang, Y. and Fan, Z. 2018. Formation of the Fe-containing intermetallic compounds during solidification of Al-5Mg-2Si-0.7Mn-1.1Fe alloy. Metallurgical and Materials Transactions A, 49: 2173-2181.

Repeto, D., Fernández-Vidal, SR., Mayuet, PF., Salguero, J. and Batista, M. 2020. On the machinability of an Al-63%SiC metal matrix composite. Materials, 13: 1-24.

Saraki, YA., Sulayman, FA. and Sulaiman, I. 2025. Characterization and experimental analysis of AA7075 aluminium alloy and rice husk ash reinforced hybrid composite. Arid Zone Journal of Engineering, Technology and Environment, 21(1): 87-100.

Corresponding author's email address: abdulgana76@yahoo.com

Sharma, AK., Bhandari, R., Sharma, C., Dhakad, S. and Pinca-Bretotean, C. 2021. A study on effects of reinforcement materials in aluminum-based metal matrix composites. International Journal of Engineering Trends and Technology, 69(9): 24-28.

Sharma, SK., Gajevic, S., Sharma, LK., Pradan, R., Sharma, Y., Miletic, I. and Stojanovic, B. 2024. Progress in aluminum-based composites prepared by stir casting: mechanical and tribological properties for automotive, aerospace and military applications. Lubricants, 12(12): 1-15.

Siddappa, PN., Shivakumar, BP., Yogesha, KB., Mruthunjaya, M. and Hanamantraygouda, MB. 2017. Machinability study of Al-TiC metal matrix composite. MATEC Web of Conferences, 144: 1-14.

Srinivasan, A., Arunachalam, RM., Ramesh, S. and Senthilkumaar, JS. 2012. Machining performance study on metal matrix composites-a response surface methodology approach. American Journal of Applied Sciences, 9(4): 478-483.

Thandalam, SK., Ramanathan, S. and Sundarrajan, S. 2015. Synthesis, microstructural and mechanical properties of ex situ zircon particles reinforced metal matrix composites: a review. Journal of Materials Research and Technology, 29(3): 333-344.

Tsaknopoulos, K., Walde, C., Tsaknopoulos, D. and Cote, DL. 2022. Evolution of Fe-rich phases in thermally processed aluminum 6061 powders for AM applications. Materials, 15(17): 1-15.

VenkataSiva, SB., Ganguly, G., Srinivasarao, G. and Sahoo, KL. 2013. Machinability of aluminum metal matrix composite reinforced with in-situ ceramic composite developed from mines waste colliery shale. Materials and Manufacturing Processes, 28: 1082-1089.

Wang, Y. and Zhang, J. 2023. A review of the friction and wear behavior of particle-reinforced aluminum matrix composites. Lubricants, 11(8): 3-17.

Zhang, Y., Saravanakumar, K. and Çopuroğlu, O. 2023. Some critical reflections on the SEM-EDS microanalysis of the hydrotalcite-like phase in slag cement paste. Materials, 16(8): 1-20.

Zubairu, PT., Hassan, AB., Muriana, RA. and Musa, NA. 2021. Effect of shea nutshell ash on the mechanical properties of cast Al6061. Arid Zone Journal of Engineering, Technology and Environment, 17(1): 1-8.

Corresponding author's email address: abdulgana76@yahoo.com